

Geometrical aspects of Gigantic Magneto-Electric effect and Quantum Pump

Ryuichi Shindou^{1*}, Naoto Nagaosa^{1,2 †}

¹ *Department of Applied Physics, University of Tokyo, Bunkyo-ku, Tokyo 113-8656, Japan*

² *CERC, AIST Tsukuba Central 4, Tsukuba 305-8562, Japan*

(Received November 6, 2018)

We study the Magneto-Electric (ME) effect from the viewpoint of the Berry phase connection and quantum adiabatic charge transport. The linear response theory for the electronic polarization \vec{P}_{el} can be interpreted in terms of the flux or the fictitious magnetic field related to the Berry phase in the generalized momentum space including external parameters. An applied magnetic field modifies the spin configuration, induces adiabatic deformation of the Bloch wavefunction, and results in the electronic polarization. This provides a new mechanism for the gigantic ME effect. For a cyclic change of the applied magnetic field, even a quantized charge transport is possible.

KEYWORDS: Magneto Electric effect, macroscopic electronic polarization, spin ordering field, generalized momentum space, fictitious magnetic field, magnetic monopole, Berry phase, depolarization field

1. Introduction

The interplay between spin and charge degrees of freedom is one of the central issues in the physics of strongly correlated electronic systems. From this viewpoint, the cross correlation between these two degrees of freedom is of particular interests. The Magneto-Electric (ME) effect is a phenomenon where a finite magnetization \vec{M} appears under an applied electric field \vec{E} or an electric polarization \vec{P} is induced by an external magnetic field \vec{H} .

This effect has been studied for a long term since its theoretical prediction¹ and experimental observations² in Cr_2O_3 . A phenomenological description of this effect is given by the free energy containing $\alpha_{ij}E_iH_j$. The selection rule for the ME coefficient α_{ij} is obtained from the group theoretical considerations. In the case of antiferromagnetically ordered Cr_2O_3 , the time-reversal symmetry (R) accompanied by the spatial translation (T) is broken due its peculiar crystal structure, in contrast to usual antiferromagnets. Instead, its AF ordered phase is invariant under the product of the time-reversal symmetry (R) and the spatial inversion (I), which does not prohibit the finite matrix element α_{ij} . Furthermore, due to the several other symmetries in antiferromagnetically ordered Cr_2O_3 , there remain only the diagonal matrix elements $\alpha_{xx} = \alpha_{yy} = \alpha_{\perp}$, $\alpha_{zz} = \alpha_{\parallel}$.¹

Microscopic theories of the ME effect in Cr_2O_3 based on these phenomenological observations have been proposed.³⁻⁵ According to these theories, the applied electric field shifts the oxygen ions O^{2-} and breaks the crystallographic equivalence between several sublattices composed of Cr atoms. For example, the g-factors on two Cr sublattices differ from each other due to the crystal field produced by the shifted oxygen ions. This difference induces a finite net magnetization.³ A temperature dependence of α_{\parallel} seems to be well explained by this mechanism.^{3,5} When we trace these theories the other way

around, a microscopic origin for the *electric polarization* induced by the applied magnetic field was attributed to the displacement of the ligand anion atoms, namely the lattice displacements.

Instead, we are going to study a *Bloch electron's contribution* to the macroscopic electronic polarization (MEP) induced by the applied magnetic field. The MEP in dielectrics has been formulated only recently, since an electron's position operator is ill-defined in the Hilbert space spanned by the Bloch wavefunctions which obey the periodic Born-von Karman (BvK) boundary condition.^{7,8} In 1990s, it is gradually recognized that the MEP in ferroelectrics is the average value of the total charges transferred through the unit area in the system associated with the atomic displacement.⁸ The atomic displacement and/or lattice distortions are induced also by the external pressure, leading to the piezo-electric effects.^{9,10}

The MEP is closely related to the quantized adiabatic particle transport proposed by Thouless and Niu in the 1980s.¹¹ They considered a 1D band insulator with the periodic boundary condition. When some external parameters are deformed adiabatically, and are put back to their initial values, the particle number transferred during this cycle is quantized to be non-zero integer. This means that the MEP increases by a finite amount, even though the external parameters get back to their initial values. Recently this kind of “d.c.” responses induced by “a.c.” impulses, which are generally called Quantum Pump, are extensively studied in meso (nano)-scale systems, where a cyclic variation of a potential shape induced by the gate voltage pumps up electrons from one end to the other end of the system.¹²⁻¹⁴ However we should make a clear distinction between the Quantum Pump discussed in these mesoscale systems and that of the 1D band insulator. Namely, the former systems is an open system attached to the leads with finite S -matrix elements between two channels, while, in the latter system, the wavefunction in one end and that of the other do not overlap due to the presence of the gapped re-

*E-mail address: shindou@appi.t.u-tokyo.ac.jp.

†E-mail address: nagaosa@appi.t.u-tokyo.ac.jp

gion between them. Furthermore, in the latter system, the particle number transferred through this gapped region during a cyclic process becomes quantized in the thermodynamic limit,^{11, 15, 16} which is not the case with the mesoscale systems.

Both MEP and Quantum Pump are closely related to the Berry phase. Berry phase is the quantal phase associated with an adiabatic time-evolution of a wavefunction. Let an external parameter evolve from $\vec{\lambda}_i$ to $\vec{\lambda}$ along a path Γ .¹⁷ Then the adiabatically evolved wavefunction $|\Psi(\vec{\lambda}(t), t)\rangle$ is given as follows.

$$|\Psi(\vec{\lambda}, t)\rangle = e^{-\int_{\Gamma}^{\vec{\lambda}_i \rightarrow \vec{\lambda}(t)} \langle \Psi_{\text{inst}}(\vec{\lambda}') | \vec{\nabla}_{\vec{\lambda}'} | \Psi_{\text{inst}}(\vec{\lambda}') \rangle \cdot d\vec{\lambda}'} |\Psi_{\text{inst}}(\vec{\lambda}(t))\rangle \quad (1)$$

where $|\Psi_{\text{inst}}(\vec{\lambda})\rangle$ is an instantaneous eigenstate of the corresponding Hamiltonian $\hat{H}(\vec{\lambda})$, and we take an initial wavefunction $|\Psi(\vec{\lambda}(t_i) \equiv \vec{\lambda}_i, t_i)\rangle$ as $|\Psi_{\text{inst}}(\vec{\lambda}_i)\rangle$. The r.h.s. of eq.(1) is invariant under the U(1) gauge transformation; $|\Psi_{\text{inst}}(\vec{\lambda})\rangle \rightarrow e^{i\theta(\vec{\lambda})} |\tilde{\Psi}_{\text{inst}}(\vec{\lambda})\rangle$ where $\theta(\vec{\lambda}_i) = 0$. Furthermore, when this parameter evolves along a closed loop Γ_{cyc} , a total phase factor this w.f. acquires, which is called U(1) phase holonomy, can be given by the surface-integral of the *flux* over an arbitrary surface S whose boundary is the loop Γ_{cyc} ;

$$e^{-\oint_{\Gamma_{\text{cyc}}} \langle \Psi_{\text{inst}}(\vec{\lambda}) | \vec{\nabla}_{\vec{\lambda}} | \Psi_{\text{inst}}(\vec{\lambda}) \rangle \cdot d\vec{\lambda}} = e^{-i \int_S \vec{B}(\vec{\lambda}) \cdot d\vec{S}},$$

where the flux $\vec{B}(\vec{\lambda})$ is defined as follows;

$$\vec{B}(\vec{\lambda}) \equiv -i \vec{\nabla}_{\vec{\lambda}} \times \langle \Psi_{\text{inst}}(\vec{\lambda}) | \vec{\nabla}_{\vec{\lambda}} | \Psi_{\text{inst}}(\vec{\lambda}) \rangle. \quad (2)$$

Since this flux is independent of the gauge choice of the instantaneous eigenstate, $\vec{B}(\vec{\lambda})$ is also called *fictitious magnetic field*, while $\vec{A}(\vec{\lambda}) \equiv \langle \Psi_{\text{inst}}(\vec{\lambda}) | \vec{\nabla}_{\vec{\lambda}} | \Psi_{\text{inst}}(\vec{\lambda}) \rangle$ corresponds to its associated vector potential.

This kind of the flux also appears in the context of the MEP and/or the Quantum Pump, since the current is represented by the derivative of the phase of the wavefunctions. Specifically the integrated particle current can be viewed as the flux penetrating a plaquette spanned by the crystal momentum and the external parameter. Although this definition of the flux is slightly modified from that of eq.(2) (see eqs.(11,12)), both of these are essentially the same mathematical objects, which are called field strengths in the framework of the gauge theory. Furthermore, the point where the energy degeneracy occurs plays a role of the source of the flux, so called, magnetic monopole (fictitious magnetic charge). Generally speaking, a magnetic monopole is an origin of nontrivial structures of the Fiber bundle associated with phase factors of wavefunctions.¹⁸

Recently the spontaneous (anomalous) Hall effect observed in ferromagnets are discussed in the context of the integer quantum Hall current from the viewpoint of the Berry phase.¹⁹ For example, the Hall conductivity σ_{xy} , is given by the total flux penetrating a plaquette spanned by x -component and y -component of the crystal momenta (2D magnetic Brillouin zone).²⁰ Throughout these extensive studies, it turned out that non-coplanar spin configurations and/or spin-orbit couplings in magnets

generate magnetic monopoles and thus nontrivial distributions of the flux in their crystal momentum spaces, which result in their anomalous Hall currents.

In this paper, we study the MEP induced by a deformation of background spin configurations in the magnetic materials. Since the spin ordering fields (external parameters) in the magnetic systems can be controlled by the applied magnetic field, this corresponds to the electronic contribution to the ME effect. As discussed above, the macroscopic electronic polarization (MEP) and the transverse conductivity σ_{xy} are closely related. Namely, these two physical quantities are the different components of the same field in the generalized momentum space. Through the analogy to the integer quantum Hall effect, we can naturally expect that even the quantized charge transport might be possible during the cyclic change of spin ordering fields. In fact, both of them are related to the first Chern numbers associated with the filled bands.

The main results obtained in this paper are summarized as follows. From the viewpoint of the perturbation theory, the Magneto-Electric (ME) effect was known to be enhanced when the energy denominator is small, i.e., when the band gap is small. However we propose, in this paper, a new mechanism of the ME effect, where not only the band gap reduction but also the U(1) phase associated with the magnetic Bloch wavefunction play very important roles in determining the magnitude of the ME effect. From this viewpoint, we can classify the magnetic dielectrics into two categories, i.e., with and without the nontrivial structure of the U(1) Fiber bundle associated with magnetic Bloch wavefunctions. Former category is a good candidate to which our mechanism can be applied. In these systems, a nontrivial topological structure is originated from the band crossing located in the parameter space. As for a specific example of this new category of magnetic dielectrics, we construct a model where such a non-trivial topological structure is realized in its generalized momentum space and gigantic electronic polarizations are induced by the applied magnetic field. In fact, their magnitudes amount to the order of $e/a^2 \sim 1$ [C/m²], where e is the electron charge and we take the lattice constant “a” to be about 4Å. A typical ME dielectric Fe₃O₄ shows an electric polarization of $\sim 1.0 \times 10^{-5}$ [C/m²] under an applied magnetic field $H = 5$ [kOe].⁶ Compared with this, the ME effect discussed in this paper has 5 orders of magnitude larger (Sec. III). Thus these electronic contribution to the ME effects can be hardly neglected compared with that of the displacement of the ligand anion atoms and so on, although the electronic contribution to the ME effects has been believed to be much smaller compared with the latter.

This paper is organized as follows. In section 2, we give our general idea for the Magneto-Electric effect (ME) based on the geometrical viewpoints and explain how the flux (fictitious magnetic field) is introduced in the context of the spin dependent MEP. In section 3, we propose a model which has a nontrivial topological structure in its generalized momentum space and exhibits a gigantic ME response. Those who want to get the overview of

this paper can skip this section. When a system is terminated without electrodes, our gigantic ME effect, as well as conventional ME effects, suffers from depolarization fields. In section.4, we give an appropriate mean-field arguments on this problems in the context of spin dependent MEP. Section 5 is devoted to conclusions.

2. Geometrical viewpoints of the spin dependent MEP

2.1 Macroscopic Electronic Polarization

In this paper, we study the change of the electronic polarization induced by a perturbation $\delta\hat{H}$ added to an original Hamiltonian \hat{H} :

$$\delta\hat{P}_{\text{el},\mu} \equiv -\frac{e}{V}(\hat{X}_{\text{el},\mu} - \langle\hat{X}_{\text{el},\mu}\rangle_{\hat{H}}). \quad (3)$$

Here $\hat{X}_{\text{el},\mu}$ is the sum of all electron's position operators and V is the volume of the system. $\langle\hat{X}_{\text{el},\mu}\rangle_{\hat{H}}$ is an expectation value of $\hat{X}_{\text{el},\mu}$ before the perturbation is introduced. According to the Kubo formula for the linear response, $\delta P_{\text{el},\mu} \equiv \langle\delta\hat{P}_{\text{el},\mu}\rangle_{\hat{H}+\delta\hat{H}}$ is given as

$$\delta P_{\text{el}} = -i\frac{e}{V} \sum_{m \neq 0} \left(\frac{\langle\Psi_0|\hat{X}_{\text{el},\mu}|\Psi_m\rangle\langle\Psi_m|\delta\hat{H}|\Psi_0\rangle}{(E_m - E_0)^2} - \text{c.c.} \right), \quad (4)$$

where $\delta\hat{H} = i[\hat{H}, \delta\hat{H}]$ and $|\Psi_m\rangle$ is an eigenstate of the Hamiltonian \hat{H} with its eigenenergy E_m . Here we assume a finite energy gap between the ground state $|\Psi_0\rangle$ and the excited state $|\Psi_m\rangle$ ($m \geq 1$) and focus on the zero-temperature case. When we transfer the time derivative from $\delta\hat{H}$ to $\hat{X}_{\text{el},\mu}$:

$$\begin{aligned} & \langle\Psi_0|\hat{X}_{\text{el},\mu}|\Psi_m\rangle\langle\Psi_m|[\hat{H}, \delta\hat{H}]\Psi_0\rangle \\ &= -\langle\Psi_0|[\hat{H}, \hat{X}_{\text{el},\mu}]\Psi_m\rangle\langle\Psi_m|\delta\hat{H}|\Psi_0\rangle, \end{aligned} \quad (5)$$

we obtain the following expression for $\delta\vec{P}_{\text{el}}$,

$$\delta P_{\text{el},\mu} = -\frac{i}{V} \sum_{m \neq 0} \left[\frac{\langle\Psi_0|\hat{J}_{\text{el},\mu}|\Psi_m\rangle\langle\Psi_m|\delta\hat{H}|\Psi_0\rangle}{(E_m - E_0)^2} - \text{c.c.} \right]. \quad (6)$$

Here we introduced an electronic current operator by $\hat{J}_{\text{el},\mu} = -ie[\hat{H}, \hat{X}_{\text{el},\mu}]$. As shown in Appendix A, this expression for the electronic polarization $\delta\vec{P}_{\text{el}}$ can be also derived as an integrated electron current over a period during which the perturbation δH is introduced. In the followings, we use eq.(6) instead of eq.(4). This is because the current operator $\hat{J}_{\text{el},\mu}$ is well-defined on a periodic lattice and thus easy to deal with, while the position operator $\hat{X}_{\text{el},\mu}$ is not.

Let the Hamiltonian depend on some external parameters $\vec{\varphi}$, i.e. $\hat{H}(\vec{\varphi})$. Then, by considering $\delta\hat{H}$ in the above formalism as $H(\vec{\varphi} + \delta\vec{\varphi}) - \hat{H}(\vec{\varphi})$, we obtain a derivative of the electronic polarization \vec{P}_{el} with respect to $\vec{\varphi}$ as

$$\frac{\partial P_{\text{el},\nu}}{\partial\varphi_\mu} = -\frac{i}{V} \sum_{m \neq 0} \left(\frac{\langle\Psi_0|\hat{J}_{\text{el},\nu}|\Psi_m\rangle\langle\Psi_m|\frac{\partial\hat{H}}{\partial\varphi_\mu}|\Psi_0\rangle}{(E_m - E_0)^2} - \text{c.c.} \right).$$

2.2 spin dependent MEP and the Flux

Now we study the spin dependent MEP. In this case, we regard $\vec{\varphi}$ as the spin ordering field $\vec{\phi}_{i,\text{SP}}$ as follows. At first we decouple the on-site Coulomb repulsion by using the Stratonovich-Hubbard field $\vec{\phi}$ and replace it by its saddle point solution $\vec{\phi}_{i,\text{SP}}$ as,

$$\begin{aligned} Z[\vec{h}] &\approx \int \mathcal{D}C^\dagger \mathcal{D}C \exp \left[-\int L(\vec{\phi}_{\text{SP}}, C^\dagger, C, \vec{h}) \right], \\ L(\vec{\phi}_{i,\text{S.P.}}, C^\dagger, C, \vec{h}) &= \\ & \frac{U}{4} \sum_i |\vec{\phi}_{i,\text{SP}}|^2 + \sum_{i,\alpha} C_{i,\alpha}^\dagger (\partial_\tau - \mu) C_{i,\alpha} + H_{\text{M.F.}} \\ H_{\text{M.F.}} &= \\ & - \sum_{i,j,\alpha} t_{ij} C_{i,\alpha}^\dagger C_{j,\alpha} + \frac{U}{2} \sum_{i,\alpha\beta} \vec{\phi}_{i,\text{SP}} \cdot C_{i,\alpha}^\dagger [\vec{\sigma}]_{\alpha\beta} C_{i,\beta} \\ & \quad + \vec{h} \cdot C_{i,\alpha}^\dagger [\vec{\sigma}]_{\alpha\beta} C_{i,\beta}, \end{aligned} \quad (8)$$

where $[\sigma_\nu]$ ($\nu = x, y, z$) are the 2×2 Pauli matrices. This saddle-point approximation is nothing but the mean field theory and we identify this saddle point solution $\vec{\phi}_{i,\text{SP}}$ with the spin ordering field. We can control this spin ordering field by changing \vec{h} . Since the saddle-point solution is determined as a function of an applied magnetic field (\vec{h}). We study the MEP induced by an adiabatic deformation of this spin ordering field $\vec{\phi}_{i,\text{SP}}$, which we will call $\vec{\varphi}$ in the followings.

When we consider a commensurate magnetic order, the wavefunction of an electronic state is given by the Slater determinant composed by the magnetic Bloch wavefunctions;

$$\langle\vec{R}_l, a, \mu, \alpha | \Phi_{n,\vec{k},\vec{\varphi}}\rangle = e^{i\vec{k}\cdot\vec{R}_l} \langle a, \mu, \alpha | n \rangle, \quad (9)$$

where $\langle a, \mu, \alpha | n \rangle \equiv \langle a, \mu, \alpha | n(\vec{k}, \vec{\varphi}) \rangle$ denotes a periodic part of the magnetic Bloch wavefunction and \vec{R}_l, a, μ and α represent the magnetic unit cell, the sublattice, orbital and spin index, respectively. By using this single-particle magnetic Bloch wavefunction, the electric linear response given in eq.(7) reduces to a more compact form in terms of Thouless-Kohmoto-Nightingale-Nijs (TKNN) formula,²⁰

$$\begin{aligned} \frac{\partial P_{\text{el},\mu}}{\partial\vec{\varphi}} \cdot \delta\vec{\varphi} &= -ie \sum_{n:\text{V.B.}} \sum_{m:\text{C.B.}} \frac{1}{(2\pi)^d} \int_{\text{M.B.Z.}} d\vec{k} \\ & \times \left(\frac{\langle n | \frac{\partial H_{\text{M.F.}}(\vec{k}, \vec{\varphi})}{\partial k_\mu} | m \rangle \langle m | \frac{\partial H_{\text{M.F.}}(\vec{k}, \vec{\varphi})}{\partial \vec{\varphi}} | n \rangle}{(\epsilon_m - \epsilon_n)^2} - \text{c.c.} \right) \cdot \delta\vec{\varphi}, \\ &= -ie \sum_{n:\text{V.B.}} \frac{1}{(2\pi)^d} \int_{\text{M.B.Z.}} d\vec{k} \left(\left\langle \frac{\partial n}{\partial k_\mu} \middle| \frac{\partial n}{\partial \vec{\varphi}} \right\rangle - \text{c.c.} \right) \cdot \delta\vec{\varphi} \end{aligned} \quad (10)$$

where $H(\vec{k}, \vec{\varphi})$ is the Hamiltonian in the momentum representation and the periodic part of the Bloch w.f. $|n\rangle \equiv |n(\vec{k}, \vec{\varphi})\rangle$ is its eigenvector with an eigenenergy $\epsilon_n \equiv \epsilon_n(\vec{k}, \vec{\varphi})$. The inner product between $\left| \frac{\partial n}{\partial k_\mu} \right\rangle \equiv \frac{\partial}{\partial k_\mu} \left(|n(\vec{k}, \vec{\varphi})\rangle \right)$ and $\left| \frac{\partial n}{\partial \varphi_\nu} \right\rangle$ denotes the contraction over sublattice, orbital and spin indices, i.e. $\sum_{a,\mu,\alpha} \left(\frac{\partial}{\partial k_\mu} \langle n(\vec{k}, \vec{\varphi}) | a, \mu, \alpha \rangle \right) \left(\frac{\partial}{\partial \varphi_\nu} \langle a, \mu, \alpha | n(\vec{k}, \vec{\varphi}) \rangle \right)$. Here

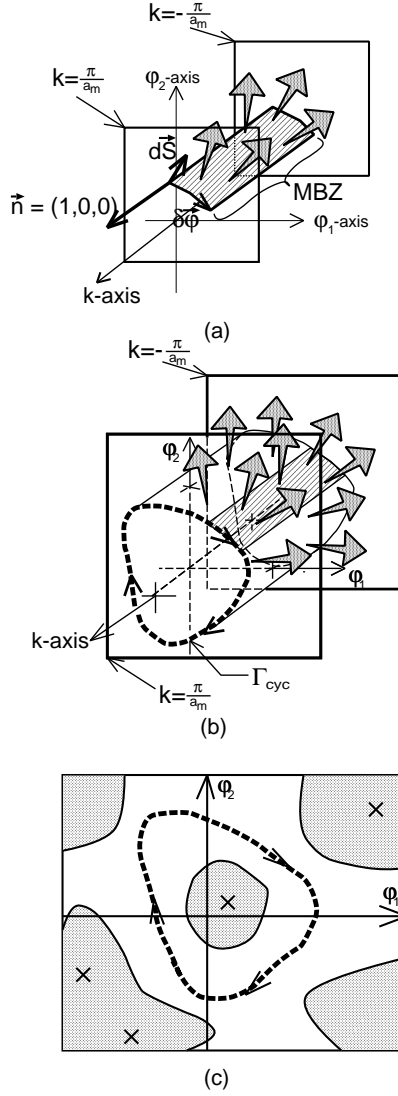


Fig. 1. (a) A shadowed rectangular area is spanned by $\delta\vec{\varphi}$ and the line parallel to k -axis, i.e., $\delta\vec{\varphi} \times [-\frac{\pi}{a_m}, \frac{\pi}{a_m}]$. \vec{n} , $\delta\vec{\varphi}$ and $d\vec{S}$ form the right hand coordinate. The gray arrows represent the flux defined in eq.(11). (b) A cyclic deformation of the external parameters $\vec{\varphi}$ in $\varphi_1 - \varphi_2$ space is defined by Γ_{cyc} . (c) Shaded regions are unphysical parameter regions (metallic regions) where a band gap closes, while, the white area denotes a gapped region. A cross (\times) denotes the parameter point where the H.V.B. and L.C.B. forms doubly degenerate point (magnetic monopole). These parameter points are included in the metallic regions. The MEP induced by the adiabatic change in the gapped region (denoted by broken line) is governed by the doubly degenerate points located in the metallic region.

the abbreviation ‘‘C.B.’’, ‘‘V.B.’’ and ‘‘M.B.Z.’’ represent the conduction bands, the valence bands and the magnetic Brillouin zone, respectively.

When we take $\vec{\varphi}$ as a two-component vector, i.e. $\vec{\varphi} = (\varphi_1, \varphi_2)$, and consider the one-dimensional system, we can introduce a 3-dimensional *generalized momentum space* spanned by the crystal momentum k and these external parameters φ_1 and φ_2 . In the following, the range of the magnetic Brillouin zone (M.B.Z.) is denoted as $[-\frac{\pi}{a_m}, \frac{\pi}{a_m}]$, where a_m is a lattice constant of the magnetic unit cell. In this generalized momentum space, we next introduce the following vector fields for each energy

band n ,

$$\vec{B}_n(k, \varphi_1, \varphi_2) = \vec{\nabla} \times \vec{A}_n(k, \varphi_1, \varphi_2), \quad (11)$$

$$\vec{A}_n(k, \varphi_1, \varphi_2) = -i \langle n(k, \varphi_1, \varphi_2) | \vec{\nabla} | n(k, \varphi_1, \varphi_2) \rangle \quad (12)$$

where $\vec{\nabla} \equiv (\partial_k, \partial_{\varphi_1}, \partial_{\varphi_2})$. This vector field $\vec{B}_n(k, \varphi_1, \varphi_2)$ is independent of the following U(1) gauge transformation of the magnetic Bloch wavefunction,

$$\begin{aligned} & \langle a, \mu, \alpha | n, k, \varphi_1, \varphi_2 \rangle \\ & \rightarrow e^{i\xi(k, \varphi_1, \varphi_2)} \langle a, \mu, \alpha | n, k, \varphi_1, \varphi_2 \rangle, \end{aligned} \quad (13)$$

while $\vec{A}_n(k, \varphi_1, \varphi_2)$ changes by $\vec{\nabla} \xi(k, \varphi_1, \varphi_2)$. Accordingly, we call $\vec{B}_n(k, \varphi_1, \varphi_2)$ and $\vec{A}_n(k, \varphi_1, \varphi_2)$ as the flux and gauge field, respectively. By using these vector fields, eq.(10) can be expressed as a surface integral of the flux over the rectangular surface spanned by $\delta\vec{\varphi}$ and the k -axis, which is drawn as the shadowed region in Fig.1(a),

$$\frac{\partial P_{\text{el}}}{\partial \vec{\varphi}} \cdot \delta\vec{\varphi} = \frac{e}{2\pi} \sum_{n: \text{V.B.}} \int_{\delta\vec{\varphi} \times [-\frac{\pi}{a_m}, \frac{\pi}{a_m}]} d\vec{S} \cdot \vec{B}_n(k, \varphi_1, \varphi_2). \quad (14)$$

The direction of $d\vec{S}$ in eq.(14) is taken so that $\vec{n} - \delta\vec{\varphi} - d\vec{S}$ forms the right-hand coordinate where \vec{n} represents a unit vector along the k -axis, i.e., $\vec{n} = (1, 0, 0)$ as in Fig.1(a).

Our strategy is first (i) to reveal the distribution of the flux for every filled energy band and then (ii) to determine the *optimal* direction, $\delta\vec{\varphi}_{\text{opt}}$, which maximizes the magnetoelectric response given in eq.(14). For this purpose, we need to identify the *source* and/or *sink* of the flux, which we will discuss in the next subsection.

2.3 Dirac monopole and Quantum Pump

In the region where the flux is well-defined, i.e. the n -th band is isolated from its neighboring bands, there are neither source nor sink associated with the flux \vec{B}_n , because $\vec{\nabla} \cdot \vec{B}_n = \vec{\nabla} \cdot (\vec{\nabla} \times \vec{A}_n) = 0$. However in those points where the n -th band forms a *degeneracy* with its neighboring bands, the flux \vec{B}_n becomes ill-defined. Therefore, these degeneracy points might become sources and/or sinks of the flux.

As shown in Appendix B, when the n -th band and its neighboring band, e.g. $(n+1)$ -th band, are degenerate at $(k, \varphi_1, \varphi_2) = (k_D, \varphi_{1,D}, \varphi_{2,D})$, this degenerate point becomes in general source and/or sink for the flux \vec{B}_n (and also \vec{B}_{n+1}) with charge 2π . We will call these doubly degenerate points as magnetic (anti-)monopoles or Dirac (anti-)monopoles from now on. Near this doubly degenerate point, the effective Hamiltonian for these two bands can be in general expanded as follows ,

$$\begin{aligned} & [\mathbf{H}]_{2 \times 2}(k, \varphi_1, \varphi_2) \\ & = (\epsilon_n(k_D, \varphi_{1,D}, \varphi_{2,D}) + \vec{K} \cdot \vec{c})[\mathbf{1}] \\ & + \sum_{\mu, \nu} K_{\mu} V_{\nu, \mu} [\sigma_{\nu}], \end{aligned} \quad (15)$$

where \vec{K} is $(k - k_D, \varphi_1 - \varphi_{1,D}, \varphi_2 - \varphi_{2,D})$, and $[\sigma_{\nu}]$ are the 2×2 Pauli matrices. The vector \vec{c} is not important for our purpose, while the determinant of the 3×3 matrix V plays an important role in classifying this degeneracy

point. According to Appendix B, for the flux of the upper band ,i.e. $\vec{B}_{n+1}(k, \vec{\varphi})$, this degeneracy point acts as an anti-monopole (sink) in the case of $\det V < 0$, while as a monopole (source) in the case of $\det V > 0$. This relation is reversed for the flux of the lower band $\vec{B}_n(k, \vec{\varphi})$, i.e.

$$\vec{\nabla} \cdot \vec{B}_n = -2\pi \cdot \text{sign}(\det V) \delta^3(\vec{K}), \quad (16)$$

$$\vec{\nabla} \cdot \vec{B}_{n+1} = 2\pi \cdot \text{sign}(\det V) \delta^3(\vec{K}). \quad (17)$$

Higher order degenerate points such as fourth-fold degenerate points have also a chance to become sources and/or sinks for the flux \vec{B}_n . However it often happens that these higher order degenerate points in the 3D parameter space can be decomposed into several number of doubly degenerate points, namely, an effective Hamiltonian reduces to the direct sum of two by two matrices given in eq.(15). Therefore we will concentrate on the doubly degenerate points in the following.

Due to the nature of doubly degenerate points given in eqs.(16) and (17), when we fill both of these two bands by electrons, $\vec{B}_n(k, \vec{\varphi})$ and $\vec{B}_{n+1}(k, \vec{\varphi})$ cancel each other in the summation of the r.h.s. of eq.(14) and the degeneracy point between the n -th and $(n+1)$ -th band becomes almost irrelevant for the MEP. On the other hand, when only the lower band is filled by electrons, $\vec{B}_n(k, \vec{\varphi})$ contributes to the MEP without being cancelled by its counter part $\vec{B}_{n+1}(k, \vec{\varphi})$ and results in a gigantic linear response, where the doubly degenerate point between these two bands plays an essential role in the direction and magnitude of the MEP. Those magnetic dielectrics which belong to the latter case of the electron filling are good candidates where this mechanism becomes relevant. Based on a specific model, we will discuss in section 3 about the physical consequences of these two types of electron fillings.

When we fix the electron number per site, those parameter points at which the highest valence band (H.V.B.) and the lowest conduction band (L.C.B.) form doubly degenerate points are usually unstable points (unphysical points). This is because making a direct band gap lowers the energy of a ground state wavefunction in general. Then the spin ordering field usually takes those parameter regions where these degeneracies are lifted. We will argue later that this is indeed the case with a specific model given in section 3. What is important and nontrivial is that *the MEP induced by the adiabatic change in these gapped phase is still controlled by the doubly degenerate points hidden in its neighboring unphysical parameter points* (See Fig.1(c)).

When we deform $\vec{\varphi}$ by a finite amount and put it back to the initial value $\vec{\varphi}_i$, i.e., making a loop Γ_{cyc} in the $\varphi_1 - \varphi_2$ plane as in Fig.1(b), the total change of the electronic polarization induced by this process is the total flux penetrating the cylinder surface spanned by Γ_{cyc} and k -axis, i.e., $\Gamma_{\text{cyc}} \times [-\frac{\pi}{a_m}, \frac{\pi}{a_m}]$,

$$\begin{aligned} \Delta_{\text{cyc}} P_{\text{el}} &\equiv \oint_{\Gamma_{\text{cyc}}} \frac{\partial P_{\text{el}}}{\partial \vec{\varphi}} \cdot d\vec{\varphi}, \\ &= \frac{e}{2\pi} \sum_{n:\text{V.B.}} \int_{\Gamma_{\text{cyc}} \times [-\frac{\pi}{a_m}, \frac{\pi}{a_m}]} d\vec{S} \cdot \vec{B}_n. \end{aligned} \quad (18)$$

This is because the surface integrals of the flux \vec{B}_n over the $k = \frac{\pi}{a_m}$ plane and that over the $k = -\frac{\pi}{a_m}$ plane cancel each other due to the periodicity. Therefore, if this cylinder has some magnetic monopoles and/or anti-monopoles of \vec{B}_n inside, we have a chance to obtain a non-zero change in the MEP after this cyclic deformation along Γ_{cyc} . This kind of the ‘‘d.c.’’ response induced by the ‘‘a.c.’’ impulse is called Quantum Pump,^{11,13} since finite amounts of electrons are transported and/or *pumped* up from the one side to the other side of the system after one cycle of this adiabatic deformation.

By using eq.(16) and eq.(17), we can simplify eq.(18) into more intuitive form. Namely, when both the $(n+1)$ -th and n -th bands are filled, a pair of magnetic monopole(anti-monopole) for the $(n+1)$ -th band and anti-monopole(monopole) for the n -th band cancel each other in the summation of the r.h.s. of eq.(18). As a result of this cancellation, the degeneracy points between *filled* bands do not contribute to the $\Delta_{\text{cyc}} P_{\text{el}}$ in eq.(18). Then a finite $\Delta_{\text{cyc}} P_{\text{el}}$ is originated only from *the degeneracy points where the highest valence band (H.V.B.) and the lowest conduction band (L.C.B.) touch*. Namely, we obtain a following simple form for the quantized particle transport:

$$\Delta_{\text{cyc}} P_{\text{el}} = -e \times \sum_{i=1}^N \text{sign}(\det V_i), \quad (19)$$

where the index i represents the doubly degenerate point between the H.V.B. and the L.C.B.. N is the total number of these degenerate points. The 3×3 matrix V given in eq.(15) is defined for each doubly degenerate point and V_i denotes that of the i -th point.

If the path Γ_{cyc} is contractible into one point without confronting a metallic region where the H.V.B. and the L.C.B. form a band crossing, the left hand side of eq.(19) is trivially zero and so is $\Delta_{\text{cyc}} P_{\text{el}}$. Therefore eq.(19) indicates that we must choose the path Γ_{cyc} to be at least *noncontractible*, in order to get non-zero $\Delta_{\text{cyc}} P_{\text{el}}$.

Finally but not the least, we want to mention about the stability of the magnetic (anti-)monopole. As is evident from eq.(15), we need to tune only 3 *real*-valued parameters in order to lift the double degeneracy. Therefore, when we add another parameter φ_{perturb} and constitute a four dimensional parameter space, the double degeneracy occurs on a *line* in this 4D space. As a result of this line degeneracy appearing in the 4D parameter space, these magnetic (anti)monopoles are stable against small perturbations. We will also revisit this point in section 3, where we will generalize the 1D studies into the 2D case by introducing weak interchain hopping terms and demonstrate that the magnetic (anti)monopole observed in the 1D studies is in fact stable against this interchain hoppings.

3. Gigantic ME Effect — spin-orbit coupling model —

Based on the concept developed in section 2, we will construct a model where the *global* rotation in a spin space induces a gigantic electronic polarization. In this model, the spin-orbit coupling plays a crucial role, be-

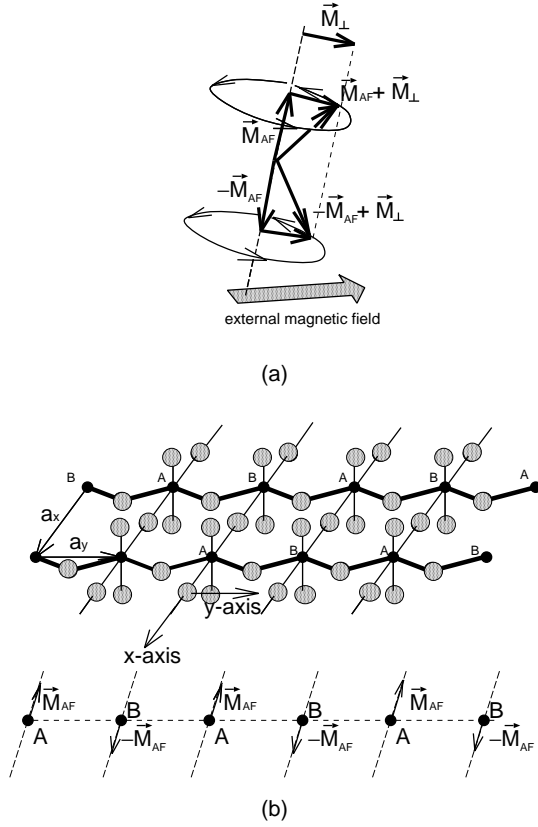


Fig. 2. (a) The sublattice magnetization $\vec{M}_{AF} + \vec{M}_{\perp}$ is for the A sublattice, while $-\vec{M}_{AF} + \vec{M}_{\perp}$ is for the B sublattice, where A and B sublattice are defined in Fig.(b). The ferromagnetic moment \vec{M}_{\perp} can be controlled by an applied magnetic field. (b) A modulated square lattice with the staggered magnetization on A and B sublattice. Grey circles denote the anion atoms while the transition metal atoms are located on the lattice. Here we draw the 1D chains extending along the y -direction by bold lines, while the interchain couplings are introduced as thin lines. Furthermore, the anion atoms on the 1D chain are shifted along the x -direction uniformly.

cause the global rotation in the spin space cannot affect its electronic state without spin-orbit interactions.

Let's consider an antiferromagnet on a modulated square lattice, where its sublattice magnetizations collinear to a particular direction (\vec{M}_{AF}) cant and acquire a ferromagnetic moment \vec{M}_{\perp} as shown in Fig.2. We can control the direction and magnitude of this ferromagnetic moment \vec{M}_{\perp} by using an external magnetic field. The hopping integral between the nearest neighbor sites depends on the intermediate anion ions, for example, oxygen O^{2-} . In Fig.2(b), we introduce the uniform shifts of the anion atoms along the x -direction, since our spin structure itself does not break the spatial inversion symmetry.

By adding an orbital index on each site in the tight binding model, we study the dielectric property of a model composed of the d -orbitals with the spin-orbit interaction and the canted antiferromagnetic order. At first, we give the result of the 1-dimensional system extending along the y -direction (bold line in the upper panel of Fig.2(b)). Next we give the 2-dimensional generalization by adding weak electron transfers along the

x -direction. This generalization will be justified, since the magnetic (anti)monopoles we will observe in the 1D studies are actually stable against small perturbations such as an interchain hopping term.

The crystal field term $H_{C.F.}$ and the kinetic energy extending along the y -direction $H_{K,y}$ are given as follows.

$$\begin{aligned}
 H_{CF} &= \sum_{i_y, \mu, \alpha} \epsilon_{\mu} C_{i_y, \mu, \alpha}^{\dagger} C_{i_y, \mu, \alpha}, \\
 H_{K,y} &= \sum_{i_y, \mu, \nu, \alpha} C_{i_y + a_y, \mu, \alpha}^{\dagger} [t^y]_{\mu\nu} C_{i_y, \nu, \alpha} + \text{c.c.}, \\
 [t^y] &= [t^{y,s}] + [t^{y,a}], \\
 &= \begin{bmatrix} -t_0 & -t_1 & 0 & 0 & 0 \\ -t_1 & -t_2 & 0 & 0 & 0 \\ 0 & 0 & -t_5 & 0 & 0 \\ 0 & 0 & 0 & -t_5 & 0 \\ 0 & 0 & 0 & 0 & 0 \end{bmatrix} \\
 &+ \begin{bmatrix} 0 & 0 & -t_3 & 0 & 0 \\ 0 & 0 & -t_4 & 0 & 0 \\ t_3 & t_4 & 0 & 0 & 0 \\ 0 & 0 & 0 & 0 & t_6 \\ 0 & 0 & 0 & -t_6 & 0 \end{bmatrix}. \quad (20)
 \end{aligned}$$

Here ϵ_{μ} is the energy of the d -orbital: $\mu = d_{x^2-y^2}, d_{3z^2-r^2}, d_{xy}, d_{yz}, d_{zx}$. The transfer integrals are composed of the symmetric parts $[t^{y,s}]$ and antisymmetric parts $[t^{y,a}]$. The antisymmetric transfer integrals t_3, t_4, t_6 result from the anion ions' shifts and their signs are reversed when the anion ions slide in the opposite direction ($-x$ direction). Namely, these transfer integrals break the spatial inversion symmetry I . Also t_1 is induced by the displacement of the anion ions. An on-site spin-orbit coupling is introduced as follows,

$$\begin{aligned}
 H_{LS} &= \sum_{\alpha, \beta, \mu, \nu} \lambda C_{i, \mu, \alpha}^{\dagger} [\vec{L}]_{\mu\nu} \cdot [\vec{\sigma}]_{\alpha\beta} C_{i, \nu, \beta}, \\
 [L_x] &= \begin{bmatrix} 0 & 0 & 0 & -i & 0 \\ 0 & 0 & 0 & -\sqrt{3}i & 0 \\ 0 & 0 & 0 & 0 & i \\ i & \sqrt{3} & 0 & 0 & 0 \\ 0 & 0 & -i & 0 & 0 \end{bmatrix}, \\
 [L_y] &= \begin{bmatrix} 0 & 0 & 0 & 0 & i \\ 0 & 0 & 0 & 0 & -\sqrt{3}i \\ 0 & 0 & 0 & i & 0 \\ 0 & 0 & -i & 0 & 0 \\ -i & \sqrt{3}i & 0 & 0 & 0 \end{bmatrix}, \\
 [L_z] &= \begin{bmatrix} 0 & 0 & 2i & 0 & 0 \\ 0 & 0 & 0 & 0 & 0 \\ -2i & 0 & 0 & 0 & 0 \\ 0 & 0 & 0 & 0 & -i \\ 0 & 0 & 0 & i & 0 \end{bmatrix}. \quad (21)
 \end{aligned}$$

As we explained in section 2, our spin ordering field, i.e. the canted AF magnetic moment, enters into our mean-field Hamiltonian in the following way:

$$H_{MF} = \frac{U}{2} \sum_{i, \mu, \alpha, \beta} \vec{\varphi}_i \cdot C_{i, \mu, \alpha}^{\dagger} [\vec{\sigma}]_{\alpha\beta} C_{i, \mu, \beta}. \quad (22)$$

Here $\vec{\varphi}_i$ is taken as $(-)\vec{M}_{AF} + \vec{M}_\perp$ when i belongs to the A(B)-sublattice. The two-component ferromagnetic moment $\vec{M}_\perp = (M_{\perp,x}, M_{\perp,y})$ can be controlled by the applied magnetic field as we mentioned above.

3.1 Odd number of electrons filling

Based on this model Hamiltonian, we consider a situation where odd number of electrons are filled per magnetic unit cell. To make the following analysis specific, we fill 3 electrons per magnetic unit cell. In order to discuss the dielectric property of this electron filling, we calculate a following flux \vec{B} :

$$\vec{B}(\vec{M}_\perp, k_y) \equiv \sum_{n=1}^3 \vec{B}_n(\vec{M}_\perp, k_y), \quad (23)$$

where a flux for each energy band, i.e. $\vec{B}_n(\vec{M}_\perp, k_y)$, is defined in eqs.(11,12), where $\vec{\nabla}$ in these equations is regarded as $(\frac{\partial}{\partial M_{\perp,x}}, \frac{\partial}{\partial M_{\perp,y}}, \frac{\partial}{\partial k_y})$ in the above equation. The crystal momentum k_y ranges $[-\frac{\pi}{2a_y}, \frac{\pi}{2a_y}]$. The distribution of this flux in the $\vec{M}_\perp - k_y$ space is given in Fig.3, where we find a source of the flux, i.e., a magnetic monopole at $(\vec{M}_\perp, k_y) = (0, 0, 0)$. This source corresponds to the doubly degenerate point which the H.V.B. ($n = 3$) and the L.C.B. ($n = 4$) form at Γ point in the case of $\vec{M}_\perp = 0$ (see Fig.4(b)). This band touching point is nothing but the Kramers doublet, since the collinear antiferromagnet ($\vec{M}_\perp = 0$) is invariant under the time-reversal operation R combined with the spatial translation by a_y ; $\{R|a_y\}$. Namely, following two Bloch wavefunctions are degenerated at $k_y = 0$ point.²¹

$$\langle a, \mu, \alpha | n, \vec{M}_\perp = 0, k_y \rangle = \sum_{b, \beta} [\sigma_x]_{ab} [-i\sigma_y]_{\alpha\beta} \langle b, \mu, \beta | n, \vec{M}_\perp = 0, -k_y \rangle \quad (24)$$

where a and b denote the sublattice index. $[\sigma_x]_{ab}$ in eq.(24) exchanges A and B sublattice and thus represents the translation by a_y . In the case of our electron-filling (3 electrons per magnetic unit cell), a finite magnetization \vec{M}_\perp always appears and lifts this degeneracy as in Fig.4(a,c). This is because making a band gap lowers the total energy of the ground state wavefunction, which we can understand by comparing the energy dispersion at $\vec{M}_\perp = 0$ and that of finite \vec{M}_\perp . (compare Fig.4(b) and (a,c)). Thereby the doubly degenerate point we mentioned above turns out to locate at an unstable parameter point. However, this degeneracy still plays an important role for the dielectric property at *finite*- \vec{M}_\perp , as we explained in section 2. Namely, even when \vec{M}_\perp is deformed within the gapped region (finite- \vec{M}_\perp region), the induced electronic polarization $P_{y,el}$ is determined by the flux $\vec{B}(\vec{M}_\perp, k_y)$ whose nontrivial distribution is originated from this doubly degenerate point at $\vec{M}_\perp = 0$. Furthermore, when \vec{M}_\perp is deformed along the path Γ_{cyc} which encloses $\vec{M}_\perp = 0$ point clockwise (Fig.3), an induced electronic polarization $\Delta_{cyc} P_{y,el}$ amounts to $+e$ due to this magnetic monopole. These features do not alter drastically as far as we fill odd number of electrons

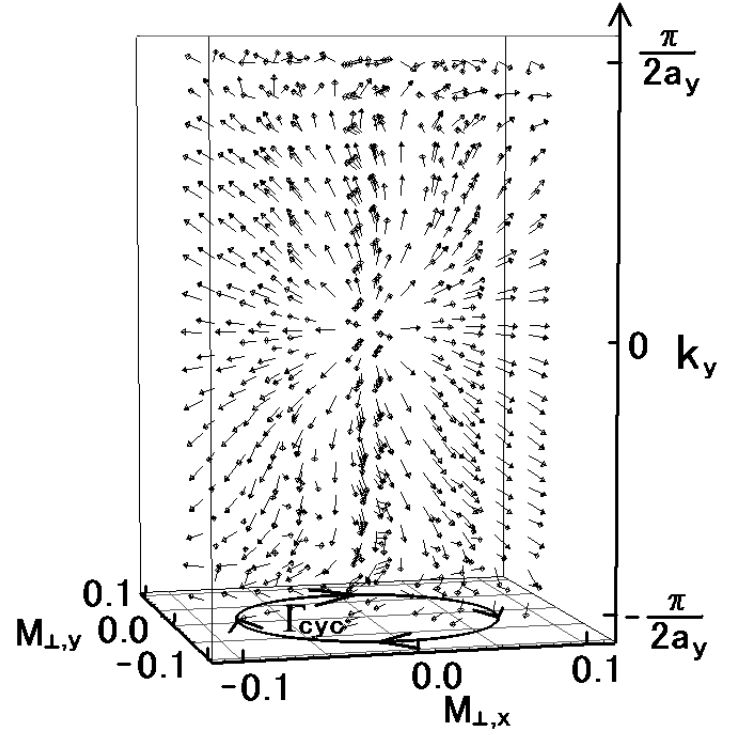


Fig. 3. A distribution of the flux \vec{B} defined in eq.(23). $t_0/U = 0.125$, $t_1/U = 0.1$, $t_2/U = 0.025$, $t_3/U = 0.075$, $t_4/U, t_5/U, t_6/U = 0.05$, $\lambda/U = 0.025$, $\epsilon_{x^2-y^2}/U = 1.25$, $\epsilon_{3z^2-r^2}/U = 1.3$, $\epsilon_{xy}/U = 0.05$, $\epsilon_{yz}/U = 0.0$, $\epsilon_{zx}/U = 0.05$, $\vec{M}_{AF} \parallel [1, 1, 1]$ and $|\vec{M}_{AF}| = 1$. We take the $M_{\perp,x}$ -axis and $M_{\perp,y}$ -axis as $(\cos \theta \cos \phi, \cos \theta \sin \phi, -\sin \theta)$ and $(-\sin \phi, \cos \phi, 0)$ respectively, where $\vec{M}_{AF} = (\sin \theta \cos \phi, \sin \theta \sin \phi, \cos \theta)$. The vertical axis of this figure is the k_y -axis whose range is taken to be $[-\frac{\pi}{2a_y}, \frac{\pi}{2a_y}]$ and we take $a_y = 10$ for visibility. We normalize the vectors to be the same in order to show only their directions.

per magnetic unit cell. Namely, we always find a magnetic monopole or antimonopole at this unstable point; $\vec{M}_\perp = 0$, which gives rise to nontrivial dielectric properties in its neighboring finite- \vec{M}_\perp regions.

3.2 Even number of electrons filling

On the contrary, when we fill even number of electrons per magnetic unit cell, e.g. 4 electrons per magnetic unit cell, the flux which describes the dielectric property, i.e., $\vec{B}(\vec{M}_\perp, k_y) \equiv \sum_{n=1}^4 \vec{B}_n(\vec{M}_\perp, k_y)$ has no significant distribution in the $\vec{M}_\perp - k_y$ space. This is because the degenerate point at $(\vec{M}_\perp, k_y) = (0, 0, 0)$ also becomes a sink of the flux \vec{B}_4 . Namely, the direction of \vec{B}_4 becomes opposite to that of \vec{B}_3 and these two flux strongly set off each other. As a result of this strong cancellation, the linear response $\partial P_{y,el} / \partial \vec{M}_\perp$ itself becomes very small in the finite- \vec{M}_\perp regions. Furthermore, the quantum pump does not occur even when \vec{M}_\perp is deformed around an $\vec{M} = 0$ point. This is because, at around $\vec{M} = 0$, there always remains a finite band gap between the H.V.B. ($n = 4$) and L.C.B. ($n = 5$).

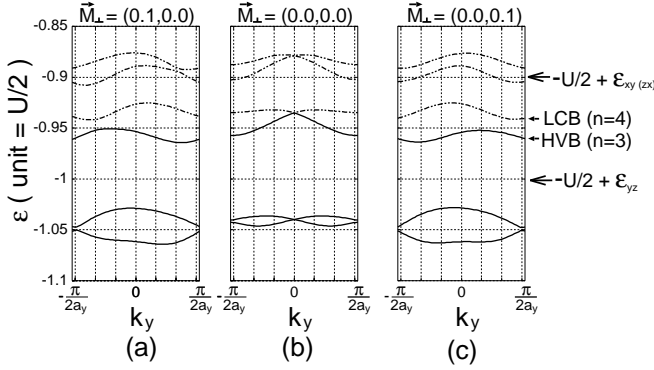


Fig. 4. Energy dispersions of the lower 6 bands, which are mainly composed of t_{2g} orbitals and constitute the lower Hubbard bands. Here we take the same parameter values as those in Fig.3. The broken lines denote those of the empty bands, while the solid lines represent the filled bands (in the case of 3 electrons per magnetic unit cell).

3.3 2-dimensional generalization

Let us generalize the above 1D studies into the 2D case with 3 electrons per magnetic unit cell. We introduce the interchain hopping integrals,

$$H_{K,x} = \Delta \sum_{\mu,\nu} C_{i_x+a_x, i_y, \mu, \alpha}^\dagger [t^{x,s}]_{\mu\nu} C_{i_x, i_y, \nu, \alpha} + \text{c.c.},$$

$$[t^{x,s}] = \begin{bmatrix} -t_0 & t_1 & 0 & 0 & 0 \\ t_1 & -t_2 & 0 & 0 & 0 \\ 0 & 0 & -t_5 & 0 & 0 \\ 0 & 0 & 0 & 0 & 0 \\ 0 & 0 & 0 & 0 & -t_5 \end{bmatrix}. \quad (25)$$

Here we ignore the antisymmetric transfer integrals coming from the anion ions' shifts, because they do not change the conclusion essentially as long as they are not so strong. Δ represents the anisotropy in transfer integrals between x - and y -directions. Then the y -component of electronic polarizations $\partial P_{y,\text{el}}/\partial \vec{M}_\perp$ in eq.(10) requires another integral with respect to the crystal momentum k_x :

$$\frac{\partial P_{y,\text{el}}}{\partial \vec{M}_\perp} \cdot \delta \vec{M}_\perp = \int_{-\frac{\pi}{2a_x}}^{\frac{\pi}{2a_x}} \frac{dk_x}{2\pi} \frac{\partial P_{y,\text{el}}(k_x)}{\partial \vec{M}_\perp} \cdot \delta \vec{M}_\perp, \quad (26)$$

$$\frac{\partial P_{y,\text{el}}(k_x)}{\partial \vec{M}_\perp} = \int_{-\frac{\pi}{2a_y}}^{\frac{\pi}{2a_y}} dk_y \sum_{n=1}^3 \sum_{\mu=x,y} \times$$

$$\left(\frac{\partial}{\partial k_y} \langle n(\vec{M}_\perp, \vec{k}) | \frac{\partial}{\partial M_{\perp,\mu}} | n(\vec{M}_\perp, \vec{k}) \rangle - \text{c.c.} \right) \delta M_{\perp,\mu},$$

$$= \frac{e}{2\pi} \sum_{n=1}^3 \int_{\delta \vec{M}_\perp \times [-\frac{\pi}{2a_y}, \frac{\pi}{2a_y}]} d\vec{S} \cdot \vec{B}_n(\vec{M}_\perp, \vec{k}). \quad (27)$$

In the followings, we will argue that $\partial P_{y,\text{el}}/\partial \vec{M}_\perp$ given in eq.(26) will exhibit quite similar behaviors as that of the previous 1D case, as far as the anisotropy parameter Δ is taken to be small.

When we constitute a four dimensional parameter space spanned by k_x, k_y and \vec{M}_\perp , the doubly degenerate *point* we have observed in the $\vec{M}_\perp - k_y$ space (see Fig.3) is expected to form a degenerate *line* in this 4D

parameter space. This is because only 3 real-valued parameters are sufficient to lift a two fold degeneracy of an hermite Hamiltonian. In the context of our model calculations, finite k_y , $M_{\perp,x}$ and $M_{\perp,y}$ have already lifted the double degeneracy and thus a new axis, i.e. k_x -axis, cannot lift this degeneracy. In fact, a simple analysis given in Appendix C proves that the double degeneracy occurs exactly on the line $\vec{M}_\perp = k_y = 0$ in this 4D parameter space.

As a result of this line degeneracy, the flux for every k_x , i.e. $\sum_{n=1}^3 \vec{B}_n(\vec{M}_\perp, k_x, k_y)$, and its integral over the surface $\delta \vec{M}_\perp \times [-\frac{\pi}{2a_y}, \frac{\pi}{2a_y}]$, i.e. $\partial P_{y,\text{el}}(k_x)/\partial \vec{M}_\perp$ exhibit a similar behaviour as that of $\sum_{n=1}^3 \vec{B}_n(\vec{M}_\perp, k_y)$ and $\partial P_{\text{el}}/\partial \vec{M}_\perp$ in the previous 1D studies. This is because, for every $k_x = \text{constant}$ space (a 3D space spanned by k_y and \vec{M}_\perp), we always find the doubly degenerate point at $(\vec{M}_\perp, k_y) = (0, 0, 0)$, which becomes a source for $\sum_{n=1}^3 \vec{B}_n(\vec{M}_\perp, k_x, k_y)$.

After taking the integral of $\partial P_{y,\text{el}}(k_x)/\partial \vec{M}_\perp$ over k_x , we calculated the electronic polarization numerically, which is shown in Fig.5. At the center of the flow diagram shown in Fig.5(a), we find the vortex, which results from the doubly degenerate line we mentioned above. In fact, the contour integral of this vector field around an arbitrary loop Γ_{cyc} enclosing this vortex clockwise produces $+e/a_x$, where the factor $1/a_x$ comes from the integral over k_x in eq.(26).

When it comes to the magnitude of $\partial P_{y,\text{el}}/\partial \vec{M}_\perp$, it becomes larger when the direct energy gap becomes smaller. For example, we show the behavior of $\partial P_{y,\text{el}}(|\vec{M}_\perp|, \theta)/\partial \theta$ as a function of θ for several constant $|\vec{M}_\perp|$ in Fig.5(b), where θ is defined as $(M_{\perp,x}, M_{\perp,y}) = |\vec{M}_\perp|(-\cos \theta, \sin \theta)$. In this figure, we can see that $\partial P_{y,\text{el}}(|\vec{M}_\perp|, \theta)/\partial \theta$ enhances around $\theta = 0.5 \sim 0.6$ in the case of $|\vec{M}_\perp| = 0.2$. This enhancement is actually accompanied by the reduction of the direct band gap.

When we stack this 2D system in the z -direction with weak interlayer couplings, the magnitude of $\partial P_{y,\text{el}}/\partial \theta$ amounts to $1 [\text{C}/\text{m}^2]$ in the case of $a = 4\text{\AA}$:

$$\frac{\partial P_{y,\text{el}}}{\partial \theta} \simeq \frac{e}{a^2}. \quad (28)$$

Meanwhile the electronic energy gain in the presence of the finite ferromagnetic moment \vec{M}_\perp (see Fig.4) is phenomenologically ascribed to the symmetric part of an anisotropic exchange interactions such as $\sum_{i,\mu=x,y,z} \Delta J_\mu S_{i,\mu} S_{i+1,\mu}$.²² Thus, as far as the linear response is concerned, we can roughly estimate the magnetic field required to rotate the spin ordering field as follows:

$$\frac{\partial \theta}{\partial h} \simeq \frac{g\mu_B}{|\Delta J|}. \quad (29)$$

Accordingly, in combination with eq.(28), the *magneto-electric coefficient* in our model turns out to amount to $10^{-3} [\text{C}/\text{m}^2 \cdot \text{kOe}]$ even in the case of $|\Delta J| = 10\text{meV}$. This value is in fact much larger than the typical value $\simeq 2 \times 10^{-6} [\text{C}/\text{m}^2 \cdot \text{kOe}]$ of the conventional magneto-electric materials. On the other hand, when the applied magnetic field is sufficiently large compared with this

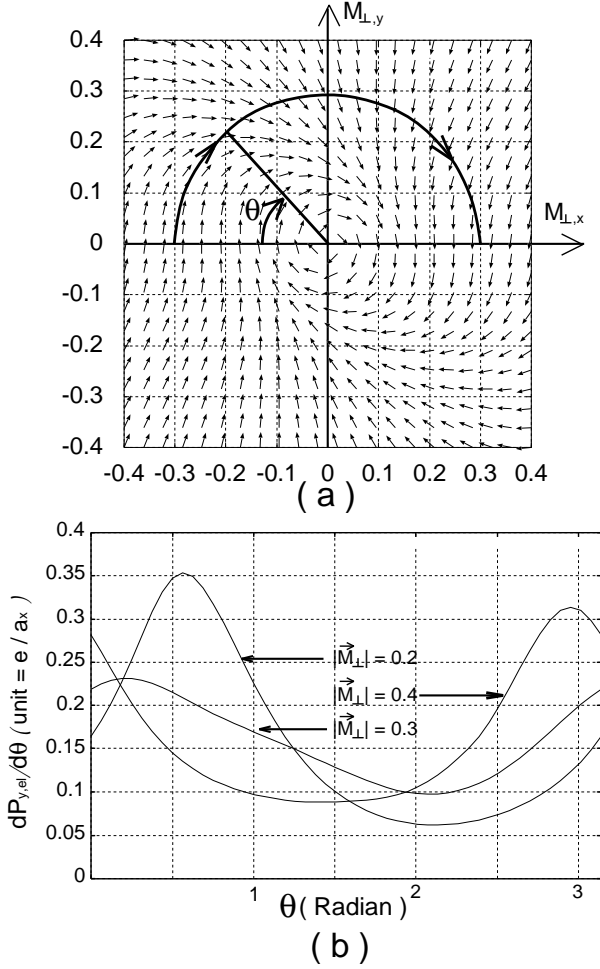


Fig. 5. (a) The flow of $dP_y(\vec{M}_\perp)/d\vec{M}_\perp$ in the 2D case. Here we take $\Delta = 0.2$. The other parameters are taken to be same as those of Fig.3. Here the magnitudes of the vectors are normalized to be same, while the informations on their magnitudes are partly given in fig.(b). (b) $dP_y(|\vec{M}_\perp|, \theta)/d\theta$ as a function of θ , where θ is defined in the text.

anisotropic exchange interactions²³ ($g\mu_B h \gg |\Delta J|$), our canted component \vec{M}_\perp follows the direction of the applied field, namely $\vec{M}_\perp // \vec{h}$.

Finally, we want to mention about the relation between the dielectric property in our models and the conventional magneto-electric (ME) effect. In the conventional ME materials, breaking the IR symmetry by applied magnetic fields induce a finite electric polarization. In our case, on the other hand, the electric polarization is allowed over the entire region in Fig.5(a). Namely, our model with the anion atoms shifted uniformly already breaks both the spatial inversion symmetry I and its combination with the time-reversal symmetry IR . However we might call this phenomenon ME effect in a wider sense, since an applied magnetic field produces an interesting electric response where a cyclic deformation of the background spin configuration pumps up electrons toward a particular direction.

4. depolarization fields - mean-field arguments -

Before rushing to concluding remarks, we want to think over the effect of depolarization fields on our

new mechanism of gigantic Magneto-Electric (ME) effect. Namely, throughout this article, we have been assuming implicitly that our system is embedded into a closed circuit, where electronic charges transported from one end to the other are always short-circuited. However, when the system is *terminated without electrodes*, the electrons accumulating at one boundary cause an electro-static potential inside the system, which seems to push back valence band electrons into the system. Speaking more generally, when an electric polarization is not short-circuited, polarized charges inside the system always induce an electric field in the direction *reverse* to this electric polarization. Thereby one might naturally expect that this *depolarization* field strongly reduces the Berry phase contributions of magneto-electric responses we have discussed so far.²⁴ In this section, we will argue how the magneto-electric response given in eq. (10,14) are suppressed in the presence of depolarization field, by taking it into account at the mean-field level.

A depolarization field induced by polarized charges is widely known to depend on a shape of the system and is sometimes complicate to figure out for an arbitrary shape.²⁵ Thus, in order to understand as simple as possible how the depolarization field affects our novel mechanism of ME effect, we will take our system to have the most simplest geometry. Namely our system is translationally invariant along y and z directions and have only two plane boundaries at $x = \pm \frac{L}{2}$. Then we can take it for granted that both an electric polarization and the depolarization field induced by polarized charges are always parallel to the x -direction. This makes the following arguments simple. For example, an electric field penetrating the plane $x' = x$, which we will call as $E_d(x)$, consists of two parts. One is proportional to an areal charge density within the region $x \leq x' \leq L/2$ and the other is to that of $-L/2 \leq x' \leq x$:

$$E_d(x, \vec{\varphi}) = -\frac{Q^+(x, \vec{\varphi})}{2\epsilon_0} + \frac{Q^-(x, \vec{\varphi})}{2\epsilon_0}. \quad (30)$$

In the above equation, we have introduced the areal charge density $Q^\pm(x, \vec{\varphi})$ as follows:

$$Q^{+(-)}(x, \vec{\varphi}) \equiv \frac{1}{S} \iiint_{x \leq x' \leq \frac{L}{2} \left(-\frac{L}{2} \leq x' \leq x \right)} \langle \Psi_0(\vec{\varphi}) | N_{\vec{r}'} | \Psi_0(\vec{\varphi}) \rangle d\vec{r}' \quad (31)$$

where $N_{\vec{r}'}$ denotes the density operator at $\vec{r}' = (x', y', z')$ and S is the total area of our plane boundary.

By including the electro-static potential due to this depolarization field, we can generalize our previous mean field Hamiltonian $H_{M.F.}$, namely eq.(8), into the following form:

$$\bar{H}_{M.F.}(\vec{\varphi}) = H_{M.F.}(\vec{\varphi}) + e \sum_{j=1}^N E(x_j, \vec{\varphi}) \cdot x_j, \quad (32)$$

where x_j denotes the x -component of a position operator of the j -th electron. Correspondingly, the previous expression for the variation of the electronic polarization w.r.t. $\vec{\varphi}$, i.e. eq.(6), is modified into the following equa-

tion;

$$\delta P_{\text{el}} = -\frac{i}{V} \sum_{m \neq 0} \left[\frac{\langle \Psi_0 | J_{\text{el}} | \Psi_m \rangle \langle \Psi_m | \delta H_{\text{M.F.}} | \Psi_0 \rangle}{(E_m - E_0)^2} - \text{c.c.} \right] - \frac{ie}{V} \sum_{m \neq 0} \left[\frac{\langle \Psi_0 | J_{\text{el}} | \Psi_m \rangle \langle \Psi_m | \sum_{j=1}^N \delta E_d(x_j) \cdot x_j | \Psi_0 \rangle}{(E_m - E_0)^2} - \text{c.c.} \right]. \quad (33)$$

The first term gives the Berry phase contribution of magneto-electric effect given in eq.(10,14), while the latter term brings about a negative feedback effect on this topological contributions, which we will argue in the followings.

From eq.(30), we can easily relate $\delta E_d(x)$ appearing in the latter term of eq.(33) with a total electronic current which passes through an arbitrary unit area at $x' = x$ while the perturbation $\delta \vec{\varphi}$ is adiabatically introduced:²⁶

$$\begin{aligned} \delta E_d(x) &= -\frac{1}{\epsilon_0} \left(Q^+(x, \vec{\varphi} + \delta \vec{\varphi}) - Q^+(x, \vec{\varphi}) \right) \\ &\equiv -\frac{\bar{J}_{\text{el}}(x)}{\epsilon_0}. \end{aligned} \quad (34)$$

Namely, a total electronic charge $Q^+(x) + Q^-(x)$ is now a conserved quantity in absence of electrodes. This current $\bar{J}_{\text{el}}(x)$ is always periodic w.r.t. a magnetic primitive translation vector; $\bar{J}_{\text{el}}(x) = \bar{J}_{\text{el}}(x + a_m)$, since we have supposed that the perturbation $\delta \vec{\varphi}$ does not break the periodicity of the magnetic unit cell.²⁷ However its distribution *within a magnetic unit cell* is not necessarily uniform in general, which would make following arguments cumbersome. Thus, we assume, for sake of simplicity, that its distribution is almost uniform within the magnetic unit cell and replace the r.h.s. of eq.(34) by an electron current integrated over the x -coordinate;²⁷

$$\delta E_d(x) \approx \delta E_d \equiv -\frac{1}{\epsilon_0 L} \int_{-L/2}^{L/2} \bar{J}_{\text{el}}(x) dx. \quad (35)$$

Since this integrated charge current is nothing but the change of an electronic polarization $\delta \vec{P}_{\text{el}}$ ⁸ (see also appendix A), an electric field due to polarized charges now turns out to be proportional only to an electronic polarization;

$$\delta E_d = -\frac{1}{\epsilon_0} \delta P_{\text{el}}. \quad (36)$$

Admitting this relation between an electronic polarization and its resulting depolarization field $\delta E_d(x)$, we could rewrite eq. (33) into a following self-consistent equation for δP_{el} ;^{28,29}

$$\delta P_{\text{el}} = \frac{e}{2\pi} \sum_{n:\text{V.B.}} \int_{\delta \vec{\varphi} \times [-\frac{\pi}{a_m}, \frac{\pi}{a_m}]} d\vec{S} \cdot \vec{B}_n(k, \varphi_1, \varphi_2) - \chi \delta P_{\text{el}}. \quad (37)$$

Here we have introduced the electric susceptibility χ as

$$\begin{aligned} \chi &= -\frac{ie}{\epsilon_0 V} \sum_{m \neq 0} \left[\frac{\langle \Psi_0 | J_{\text{el}} | \Psi_m \rangle \langle \Psi_m | X_{\text{el}} | \Psi_0 \rangle}{(E_m - E_0)^2} - \text{c.c.} \right], \\ X_{\text{el}} &\equiv \sum_{j=1}^N x_j. \end{aligned}$$

The first term of the r.h.s. in eq.(37) corresponds to the Berry phase contributions to the magneto-electric

response, while the latter term gives a factor $\frac{1}{1+\chi}$ to this topological contributions. Namely, the above mean-field equation for δP_{el} gives us a following expression for the magneto-electric responses in absence of electrodes:

$$\frac{\partial P_{\text{el}}}{\partial \vec{\varphi}} \cdot \delta \vec{\varphi} = \frac{1}{1+\chi} \frac{e}{2\pi} \sum_{n:\text{V.B.}} \int_{\delta \vec{\varphi} \times [-\frac{\pi}{a_m}, \frac{\pi}{a_m}]} d\vec{S} \cdot \vec{B}_n(k, \varphi_1, \varphi_2) \quad (38)$$

The electric susceptibility χ in dielectrics ranges from 5 to 5000. Therefore, the magneto-electric coefficient we estimated in the previous section (see just below eq.(29)) decreases by factor 10^{-1} to 10^{-3} in presence of dipolarization fields. Furthermore the electric susceptibility usually becomes larger when a direct band gap smaller. Thus, in the systems terminated without electrodes, our Berry phase mechanism of gigantic ME effect seems to inevitably meet a severe reduction due to this depolarization field. Namely, when one look for those mean fields $\vec{\varphi}$ near which the H.V.B. and the L.C.B. form magnetic (anti)monopoles, not only the Berry phase contributions, i.e. $\sum_{n:\text{V.B.}} \vec{B}_n(k, \varphi_1, \varphi_2)$, but the negative feedback factor $1+\chi$ also enhances. However, when the system is terminated *with* electrodes and electronic polarizations are measured through (short-circuited) integrated currents, the system is in general free from the depolarization field mentioned in this section and thereby our Berry phase mechanism of gigantic ME effect does not suffer from its negative feedback factor.

5. Conclusion

In this article, we have studied the new mechanism for a gigantic Magneto-Electric (ME) effect. This is due to the geometrical Berry phase of the Bloch electrons, which is represented by the flux in the generalized momentum space including the external parameters such as the direction of the sublattice magnetization. We proposed a specific model, the multi-band models with the spin-orbit interaction, where a magnetic monopole and an anti-monopole appear in this generalized momentum space and determine the distribution of the flux. These (anti)monopoles are attributed to the Kramers doublet, where the broken time-reversal symmetry in addition to the broken spatial inversion symmetry is essential. This model calculation indicates that the ME effect is not simply determined by the magnitude of the energy gap, and the geometrical structure of the U(1) gauge associated with the Bloch wavefunctions also plays an important role. A comparison with the conventional ME effect⁶ suggests that the magnitude could be $\sim 10^3$ times larger when the monopole's contribution to the electronic polarization survives. Although we do not have an explicit candidate for real systems, it would be very interesting to look for the material where this mechanism of gigantic ME effect works. The detailed band structure calculations will be helpful to reveal the distribution of the flux in the generalized momentum space, which are left for future studies.

Acknowledgments

The authors acknowledge S. Ishihara, Z.Fang, T.Egami S.Murakami, M.Onoda, and Y.Tokura for fruitful discussions. This work is supported by Grant-in-Aids from the Ministry of Education, Culture, Sports, Science, and Technology of Japan.

Appendix A: the integrated electron current

In this Appendix, we will argue that the change of the electronic polarization $\delta P_{\text{el},\mu}$ given in eq.(6) is identical to a total charge transport $\bar{J}_{\text{el},\mu}$.⁸ This quantity is defined as the total current flowing through the system while the perturbation δH is adiabatically introduced from $t = -\infty$ to $t = 0$:

$$\bar{J}_{\text{el},\mu} \equiv \frac{1}{V} \int_{-\infty}^0 \langle \Psi(t) | J_{\text{el},\mu} | \Psi(t) \rangle dt. \quad (\text{A.1})$$

$$J_{\text{el},\mu} \equiv \int_V J_{\text{el},\mu}(\vec{x}) d\vec{x}$$

Here $|\Psi(t)\rangle$ is an adiabatically evolved ground state wavefunction:

$$i \frac{\partial}{\partial t} |\Psi(t)\rangle = \left[\hat{H} + \frac{1}{2} \left(\delta \hat{H} e^{i(\omega - i\delta)t} + \text{H.c.} \right) \right] |\Psi(t)\rangle. \quad (\text{A.2})$$

Therefore, in the translationally invariant systems, $\bar{J}_{\text{el},\mu}$ represents the total charges which pass through a unit area normal to the $\mu = \text{constant}$ plane while $t \in [-\infty, 0]$. According to the standard time-dependent perturbation theory, $|\Psi(t)\rangle$ can be expanded by the eigenstate $|\Psi_m\rangle$ at $t = -\infty$:

$$|\Psi(t)\rangle = |\Psi_0\rangle e^{-iE_0 t} + \sum_{m \neq 0} |\Psi_m\rangle a_m(s) e^{-iE_m t},$$

where its coefficient $a_m(t)$ reads:

$$a_m(t) = -\frac{e^{i(E_m - E_0 + \omega - i\delta)s}}{E_m - E_0 + \omega - i\delta} \langle \Psi_m | \frac{1}{2} \delta \hat{H} | \Psi_0 \rangle - \frac{e^{i(E_m - E_0 - \omega - i\delta)t}}{E_m - E_0 - \omega - i\delta} \langle \Psi_m | \frac{1}{2} \delta \hat{H} | \Psi_0 \rangle.$$

Then the electronic current density is given up to the first order in $\delta \hat{H}$ as

$$\frac{1}{V} \langle \Psi(t) | \hat{J}_{\text{el},\mu} | \Psi(t) \rangle = j_{\text{el},\mu}(\omega) e^{i(\omega - i\delta)t} + \text{c.c.}, \quad (\text{A.3})$$

$$j_{\text{el},\mu}(\omega) \equiv -\frac{1}{V} \sum_{m \neq 0} \left(\frac{\langle \Psi_0 | \hat{J}_{\text{el},\mu} | \Psi_m \rangle \langle \Psi_m | \frac{1}{2} \delta \hat{H} | \Psi_0 \rangle}{E_m - E_0 + \omega - i\delta} + \frac{\langle \Psi_m | \hat{J}_{\text{el},\mu} | \Psi_0 \rangle \langle \Psi_0 | \frac{1}{2} \delta \hat{H} | \Psi_m \rangle}{E_m - E_0 - (\omega - i\delta)} \right), \quad (\text{A.4})$$

where we omitted $\langle \Psi_0 | \hat{J}_{\text{el},\mu} | \Psi_0 \rangle$, because the system is an insulator at $t = -\infty$. Then by substituting eq.(A.3) into eq.(A.1), we obtain $\bar{J}_{\text{el},\mu}$ in the following way:

$$\bar{J}_{\text{el},\mu} = \frac{1}{i(\omega - i\delta)} (j_{\text{el},\mu}(\omega) - j_{\text{el},\mu}(\omega = 0)) + \text{c.c.} \quad (\text{A.5})$$

Here we subtracted $2\pi\delta(\omega)j_{\text{el},\mu}(\omega = 0)$ from $\bar{J}_{\text{el},\mu}$, because we assume that the system remains an insulator from $t = -\infty$ to $t = 0$. When we take the static limit ($\omega \rightarrow 0$), $\bar{J}_{\text{el},\mu}$ given in eq.(A.5) is in fact identical to $\delta \bar{P}_{\text{el}}$ given in eq.(6).

Appendix B: fictitious magnetic charge

In this Appendix, we will prove that the doubly degenerate point defined in eq.(15) is identical to the fictitious magnetic charge associated with the flux defined in eqs.(11) and (12). Namely, we will show that the surface-integral of the flux over an closed surface enclosing this doubly degenerate point becomes quantized to be $\pm 2\pi$.

First we will consider the surface-integral of the flux over an infinitesimally small box $v \equiv \{(K_x, K_y, K_z) | (K_x, K_y, K_z) \in [-\delta_x, \delta_x] \times [-\delta_y, \delta_y] \times [-\delta_z, \delta_z]\}$ enclosing this degenerate point, i.e.

$$\int \int_{\partial v} d\vec{S} \cdot \vec{B}_n(\vec{K}). \quad (\text{B.1})$$

Here we take the vector $d\vec{S}$ to be directed from inside to outside of this box. When we define a new coordinate:

$$\begin{aligned} \begin{bmatrix} K'_x \\ K'_y \\ K'_z \end{bmatrix} &= \begin{bmatrix} 1 & & \\ & \text{sign}(\det V) & \\ & & 1 \end{bmatrix} \cdot [V] \cdot \begin{bmatrix} K_x \\ K_y \\ K_z \end{bmatrix}, \\ &\equiv [T] \cdot \begin{bmatrix} K_x \\ K_y \\ K_z \end{bmatrix}, \end{aligned}$$

the 2×2 reduced Hamiltonian given in eq.(15) can be rewritten as follows,

$$[\mathbf{H}]_{2 \times 2} = K'_x [\sigma_x] + \text{sign}(\det V) \cdot K'_y [\sigma_y] + K'_z [\sigma_z], \quad (\text{B.2})$$

where we omitted those terms which are proportional to a unit matrix. Then, accompanied with this coordinate transformation, a following flux can be introduced,

$$\vec{B}'_n(\vec{K}') = -i \nabla_{\vec{K}'} \times \langle n, \vec{K}' | \vec{\nabla}_{\vec{K}'} | n, \vec{K}' \rangle, \quad (\text{B.3})$$

whose relation to the flux in the old coordinate, i.e. $\vec{B}_n(\vec{K})$, are given as follows:

$$\begin{aligned} B_{n,\mu}(\vec{K}) &= \det T \sum_{\nu} [T^{-1}]_{\mu,\nu} B'_{n,\nu}(\vec{K}'), \\ &= \sum_{\nu} \tilde{a}_{\nu,\mu} B'_{n,\nu}(\vec{K}'). \end{aligned}$$

Here $\tilde{a}_{\nu,\mu}$ denotes the (ν, μ) -th cofactor of the 3×3 matrix $[T]$.

We will show in the following that eq.(B.1) can be rewritten into the r.h.s. of eq.(B.5) below. The integral in eq.(B.1) consists of the surface-integral over the 6 rectangulars. When we focus on one of them, e.g. the rectangular $X_+ \equiv \{(K_x, K_y, K_z) | K_x = \delta_x, (K_y, K_z) \in [-\delta_y, \delta_y] \times [-\delta_z, \delta_z]\}$, the integral over this rectangular can be transformed as follows;

$$\begin{aligned} &\int \int_{X_+} dK_y dK_z B_{n,x} \\ &= \int \int_{T(X_+)} d\vec{S}' \cdot \vec{B}'_n(\vec{K}'). \end{aligned} \quad (\text{B.4})$$

Here the direction of $d\vec{S}'$ was also taken so that it penetrates the parallelogram $T(X_+)$ from inside to outside of the box $T(v)$. This relation results from the following

mathematics;

$$\begin{aligned}
& dK_y dK_z B_{n,x} \\
&= dK_y dK_z (\tilde{a}_{xx} B'_{n,x} + \tilde{a}_{yx} B'_{n,y} + \tilde{a}_{zx} B'_{n,z}), \\
&= \left(\begin{bmatrix} T_{xy} \\ T_{yy} \\ T_{zy} \end{bmatrix} dK_y \times \begin{bmatrix} T_{xz} \\ T_{yz} \\ T_{zz} \end{bmatrix} dK_z \right) \cdot \begin{bmatrix} B'_{n,x} \\ B'_{n,y} \\ B'_{n,z} \end{bmatrix}, \\
&= d\vec{S}' \cdot \vec{B}'_n,
\end{aligned}$$

where we used the fact that the parallelogram $T(X_+)$ in eq.(B-4) is spanned by $[T_{xy}, T_{yy}, T_{zy}]^t dK_y$ and $[T_{xz}, T_{yz}, T_{zz}]^t dK_z$ and that the 3×3 matrix $[T]$ is positive definite by definition. The other surface-integrals over remaining 5 faces can be also transformed in a similar way. As a result, in the K' -coordinate, eq.(B-1) reads:

$$\begin{aligned}
\text{eq.(B-1)} &= \int \int_{\partial T(v)} d\vec{S}' \cdot \vec{B}'_n(\vec{K}'), \\
&= \int \int_S d\vec{S}' \cdot \vec{B}'_n(\vec{K}'), \quad (\text{B-5})
\end{aligned}$$

where S is the sphere enclosing the origin, i.e. $\vec{K}' = 0$.

By using the spherical coordinate; $(K'_x, K'_y, K'_z) = K'(\sin \theta \cos \phi, \sin \theta \sin \phi, \cos \theta)$, the eigenvector of eq.(B-2) can be given as follows,

$$|n, \vec{K}'\rangle = \begin{cases} \begin{bmatrix} \cos \frac{\theta}{2} \\ \sin \frac{\theta}{2} e^{i\phi \cdot \text{sign}(\det V)} \\ \sin \frac{\theta}{2} e^{-i\phi \cdot \text{sign}(\det V)} \end{bmatrix}, & \text{for } E_n = K' \\ \begin{bmatrix} \cos \frac{\theta}{2} \\ \sin \frac{\theta}{2} e^{-i\phi \cdot \text{sign}(\det V)} \\ -\cos \frac{\theta}{2} \end{bmatrix}. & \text{for } E_n = -K' \end{cases}$$

Accordingly, the flux defined in eq.(B-3) can be calculated easily,

$$\begin{aligned}
\vec{B}'_n(\vec{K}') &= \frac{1}{K'^2 \sin \theta} \left(\frac{\partial}{\partial \theta} \langle n, \vec{K}' | \frac{\partial}{\partial \phi} |n, \vec{K}'\rangle - \text{c.c.} \right) \frac{\vec{K}'}{K'}, \\
&= \pm \frac{1}{2K'^2} \cdot \text{sign}(\det V), \quad (\text{B-6})
\end{aligned}$$

where the sign $+$ is for the case where the n -th band is the upper band and the $-$ sign is for the lower band. Substituting eq.(B-6) into the r.h.s. of eq.(B-5), we get

$$\begin{aligned}
& \int \int_{\partial v} d\vec{S} \cdot \vec{B}_n(\vec{K}) \\
&= \pm 2\pi \cdot \text{sign}(\det V), \quad (\text{B-7})
\end{aligned}$$

where \pm correspond to those in eq.(B-6). To summarize, in the case of $\det V < 0$, the flux for the upper band sinks into $\vec{K} = 0$, while that for the lower band streams from this origin with 2π charge. But in the case of $\det V > 0$, the above relations are reversed.

Appendix C: \vec{M}_{AF} collinear to an arbitrary direction

In this Appendix, we will argue that a double degeneracy always occurs on the line; $\vec{M}_{\perp} = k_y = 0$ in the $k_x - k_y - \vec{M}_{\perp}$ space. As we argued in eq.(24), the following two Bloch wave functions are energetically degenerated:

$$\begin{aligned}
& \langle a, \mu, \alpha | n(\vec{M}_{\perp} = 0, \vec{k}) \rangle = \\
& \sum_{b, \beta} [\sigma_x]_{ab} [-i\sigma_y]_{\alpha\beta} \langle b, \mu, \beta | n(\vec{M}_{\perp} = 0, -\vec{k}) \rangle \quad (\text{C-1})
\end{aligned}$$

since our 2D system with the collinear AF mean field is invariant under the time reversal operation combined with the spatial translation, i.e. $\{R|a_y\}$.

In addition to this, the periodic part of the Bloch function at (k_x, k_y) and that of $(-k_x, k_y)$ are identical to each other, which are also energetically degenerated:

$$\langle a, \mu, \alpha | n(\vec{M}_{\perp}, k_x, k_y) \rangle = \langle a, \mu, \alpha | n(\vec{M}_{\perp}, -k_x, k_y) \rangle. \quad (\text{C-2})$$

We can easily verify eq.(C-2), when we write down our Hamiltonian in the momentum representation: $\sum [H(\vec{k}, \vec{M}_{\perp})]_{(a, \mu, \alpha | b, \nu, \beta)} f_{\vec{k}, a, \mu, \alpha}^{\dagger} f_{\vec{k}, b, \nu, \beta}$. Namely, $[H(\vec{k}, \vec{M}_{\perp})]$ is composed from the following five parts:

$$\begin{aligned}
[H] &= [H_{\text{CF}}] + [H_{\text{K},y}] + [H_{\text{LS}}] + [H_{\text{MF}}] + [H_{\text{K},x}], \\
[H_{\text{CF}}] &= \epsilon_{\mu} \delta_{ab} \delta_{\mu\nu} \delta_{\alpha\beta}, \\
[H_{\text{K},y}] &= 2 \cos(k_y a_y) [\sigma_x]_{ab} [\mathbf{t}^{y,s}]_{\mu\nu} \delta_{\alpha\beta} \\
&\quad + 2 \sin(k_y a_y) [\sigma_y]_{ab} [\mathbf{t}^{y,a}]_{\mu\nu} \delta_{\alpha\beta}, \\
[H_{\text{LS}}] &= \sum_{\lambda=x,y,z} \delta_{ab} [\mathbf{L}\lambda]_{\mu\nu} [\sigma\lambda]_{\alpha\beta}, \\
[H_{\text{MF}}] &= \sum_{\lambda} \left\{ (\vec{M}_{\text{AF}})_{\lambda} [\sigma_z]_{ab} + (\vec{M}_{\perp})_{\lambda} \delta_{ab} \right\} \delta_{\mu\nu} [\sigma\lambda]_{\alpha\beta}, \\
[H_{\text{K},x}] &= 2\Delta \cos(k_x a_x) [\sigma_x]_{ab} [\mathbf{t}^{x,s}]_{\mu\nu} \delta_{\alpha\beta},
\end{aligned}$$

where a, b denote the sublattice indice and μ, ν and α, β are those for the orbital and spin respectively. Since we didn't take into account the *antisymmetric* transfer integrals along the x -direction, $[H(\vec{k}, \vec{M}_{\perp})]$ is clearly invariant under the sign change of k_x . Therefore its eigenvector at (k_x, k_y) is identical to that of $(-k_x, k_y)$.

Eqs.(C-1,C-2) indicate that the following two Bloch functions are energetically degenerated along $k_y = 0$ when the ferromagnetic moment vanishes ($\vec{M}_{\perp} = 0$);

$$\begin{aligned}
& \langle a, \mu, \alpha | n(\vec{M}_{\perp} = 0, k_x, k_y) \rangle = \\
& \sum_{b, \beta} [\sigma_x]_{ab} [-i\sigma_y]_{\alpha\beta} \langle b, \mu, \beta | n(\vec{M}_{\perp} = 0, k_x, -k_y) \rangle
\end{aligned}$$

Appendix D: \vec{M}_{AF} collinear to the z -direction

In this Appendix, we will argue that when \vec{M}_{AF} is collinear to the z -direction, another double degeneracy occurs at X point, i.e. $(k_x, k_y) = (\frac{\pi}{2a_x}, \pm \frac{\pi}{2a_y}) \equiv \vec{k}_X$, irrespective of \vec{M}_{\perp} . Namely, a doubly degenerate surface appears in the 4D parameter space spanned by k_x, k_y and \vec{M}_{\perp} .

When $\vec{M}_{\perp} = 0$ with \vec{M}_{AF} collinear to the z -direction, the system is invariant under the following symmetry operations;

$$E, \{\sigma_y|a_y\}, IC_{2z}, \{C_{2x}|a_y\},$$

in addition to $\{R|a_y\}$. Here I, σ_y and $C_{2x(z)}$ represent the spatial inversion, mirror with respect to the $y = 0$ plane and the spatial rotation by π around the $x(z)$ -axis respectively. Then the k -group at X point is composed of a unitary subgroup $G_X \equiv T_{\vec{R}_l} \times \{E, IC_{2z}\}$ and an anti-unitary subgroup $\{R|a_y\} \times T_{\vec{R}_l} \times \{E, IC_{2z}\}$. $T_{\vec{R}_l}$ denotes the spatial translation by $\vec{R}_l \equiv n(a_x + a_y) + m(a_x - a_y)$, where n and m take an arbitrary integer. Then the irreducible

representation of the unitary subgroup $T_{\vec{R}_l} \times \{E, IC_{2z}\}$ becomes $e^{i\vec{k}_X \cdot \vec{R}_l} \Gamma_{C_{1h}}(\{E, IC_{2z}\})$, where $\Gamma_{C_{1h}}$ denotes the representation of the monoclinic point group C_{1h} . The character table for the monoclinic point group is given in Table.I, where we only take the double-valued rep-

C_{1h}	E	E	IC_{2z}	IC_{2z}
Γ_3	1	-1	$-i$	i
Γ_4	1	-1	i	$-i$

Table D-1. Character table for double-valued representation of the monoclinic point group C_{1h} . $IC_{2z} \equiv \bar{E}IC_{2z}$

resentation since we treat the spinful Hamiltonian with spin-orbit interactions. \bar{E} in Table.I represents the 2π rotation in the spin- $\frac{1}{2}$ space whose character is always -1 . The dimensionality of these two representation are doubled due to the presence of the anti-unitary subgroup, $\{R|a_y\} \times T_{\vec{R}_l} \times \{E, IC_{2z}\}$. Namely, since the Wigner's criterion³⁰ reads

$$\begin{aligned} & \sum_{u \in G_X, \bar{E}G_X} \chi^X(\{R|\vec{a}_y\} \cdot u)^2 \\ &= 2 \sum_{\vec{R}_l} e^{2i\vec{k}_X \cdot (\vec{a}_y + \vec{R}_l)} \left(\Gamma_{C_{1h}}(R^2) + \Gamma_{C_{1h}}(R^2 C_{2z}^2) \right), \\ &= 2 \sum_{\vec{R}_l} e^{2i\vec{k}_X \cdot (\vec{a}_y + \vec{R}_l)} (\Gamma_{C_{1h}}(\bar{E}) + \Gamma_{C_{1h}}(E)) = \mathbf{0} \cdot \mathbf{1} \end{aligned}$$

only 2-dimensional representations are allowed at X point irrespective of whether $\Gamma_{C_{1h}}$ is chosen to be Γ_3 or Γ_4 . Here χ^X in eq.(D-1) denotes the character of the irreducible representation of the k -group at X -point.

These degeneracies still remain even when we violate the time-reversal symmetry $\{R|a_y\}$ by introducing finite \vec{M}_\perp . In the case of $\vec{M}_\perp \neq 0$, the system is still invariant under the $T_{\vec{R}_l} \times \{E, \{RIC_{2z}|a_y\}\}$. Then the degeneracy at X point becomes doubled due to its anti-unitary element $\{RIC_{2z}|a_y\}$:

$$\begin{aligned} & \sum_{u = T_{\vec{R}_l} \times \{E, \bar{E}\}} \chi^X(\{RIC_{2z}|a_y\} \cdot u)^2 \\ &= 2 \sum_{\vec{R}_l} e^{2i\vec{k}_X \cdot (\vec{R}_l + \vec{a}_y)} = -2N, \end{aligned}$$

where $2N$ is the total number of the elements of the unitary k -group $T_{\vec{R}_l} \times \{E, \bar{E}\}$. To summarize, we always have a double degeneracy at X point regardless of \vec{M}_\perp .

- 1) I.E.Dzyaloshinskii, Sov. Phys. JETP, **10**, 628 (1960)
- 2) G.T.Rado and V.J. Folen, Phys.Rev.lett. **7**, 310, (1961), J.appl.Phys. **33**, 1126S (1962)
- 3) S.Alexander and S.Shtrikman, Solid State Comm. **4**, 115 (1965), R.Hornreich and S.Shtrikman, Phys. Rev. **161**, 506 (1967)
- 4) M.Date, J.Kanamori and M.Tachiki J.Phys.Soc.Japan **16**, 2569 (1961)
- 5) H.Yatom and R.Englman Phys.Rev. **188**,793 (1969)
- 6) G.T.Rado, J.M.Ferrari, Phys.Rev.B **12**, 5166 (1975)

- 7) R. D. King-Smith and D. Vanderbilt Phys. Rev. B. **47**, 1651 (1993).
- 8) R. Resta, EuroPhys. Lett. **22** 133 (1993), Rev. Mod. Phys. **55**, 899 (1994)
- 9) F. Bernardini, V. Fiorentini, and D. Vanderbilt, Phys. Rev. B **56**, R10024 (1997), L. Bellaiche and D. Vanderbilt, Phys. Rev. Lett. **83**, 1347 (1999).
- 10) J.E.Avron et al, Phys. Rev. Lett. **78**, 511 (1997).
- 11) D.J.Thouless, Phys.Rev.B **27**, 6083 (1983), Q.Niu, D.J.Thouless, J.Phys.A **17**, 2453 (1984).
- 12) M. Switkes, C. M. Marcus, K. Campman and A. C. Gossard, Science **283**, 1905 (1999)
- 13) B.L.Altshuler, L.I.Galzman, Science **283**, 1864 (1999)
- 14) P.W. Brouwer, Phys. Rev. B **58**, R10135, (1998)
- 15) Q. Niu and D. J. Thouless, J. Phys. A **17**, 2453 (1984)
- 16) R. Shindou, condmat/0312668
- 17) M.V.Berry, Proc.Roy.Soc.Lond.**A392**, 45 (1984)
- 18) M.Nakahara, *Geometry, topology and physics* (Institute of Physics Publishing, 1990)
- 19) K.Ohgushi, S.Murakami and N.Nagaosa, Phys. Rev. B 62(10), R6065 (2000), Y.Taguchi, Y.Ohara, H.Yoshizawa, N.Nagaosa and Y.Tokura, Science **291**, 2573 (2001), R.Shindou and N.Nagaosa, Phys. Rev. Lett. **87** 116801 (2001), M.Onoda and N.Nagaosa, J. Phys. Soc. Jpn. **71**(1) 19 (2002)
- 20) D.J.Thouless, M.Kohmoto, M.P.Nightingale and M.den Nijs, Phys.Rev.Lett. **49**, 405 (1982), M.Kohmoto, Ann.Phys.(N.Y.) **160**, 343 (1985)
- 21) The time reversal operator acts on our Hamiltonian, $\hat{H} = H_{(i,\mu,\alpha|j,\nu,\beta)} f_{i,\mu,\alpha}^\dagger f_{j,\nu,\beta}$ in the follow way;

$$\begin{aligned} H_{(i,\mu,\alpha|j,\nu,\beta)} & \rightarrow \sum_{\mu',\mu''} \sum_{\alpha',\beta'} [R^{(t)}]_{\mu\mu'}^{-1} [\sigma_y]_{\alpha\alpha'} \\ & H_{(i,\mu',\alpha'|j,\nu',\beta')}^* [R^{(t)}]_{\nu'\nu} [-i\sigma_y]_{\beta\beta'} \end{aligned}$$

while the spatial rotation around \vec{n} by θ , i.e., $C(\vec{n}, \theta)$ acts as follows,

$$\begin{aligned} H_{(i,\mu,\alpha|j,\nu,\beta)} & \rightarrow \sum_{\mu',\mu''} \sum_{\alpha',\beta'} [e^{-i\theta\vec{n}\cdot\vec{L}}]_{\mu\mu'} [e^{-i\theta\vec{n}\cdot\vec{S}}]_{\alpha\alpha'} \\ & H_{(C(\vec{n},\theta)^{-1}(i),\mu',\alpha'|C(\vec{n},\theta)^{-1}(j),\nu',\beta')} \\ & [e^{i\theta\vec{n}\cdot\vec{L}}]_{\nu'\nu} [e^{i\theta\vec{n}\cdot\vec{S}}]_{\beta'\beta}. \end{aligned} \quad (\text{D-3})$$

Here the indice i, j are the site indice (not only magnetic unit cell indice but also sublattice indice are included), μ and ν are orbital indice and α, β are those for spin. As for the operators on the orbital space, when the basis functions for d-orbital indice μ and ν were taken as $|L^2 = 2(2+1), L_z = 2\rangle, |6, 1\rangle, |6, 0\rangle (\equiv |6, 0^*\rangle), |6, -1\rangle (\equiv |6, 1^*\rangle), |6, -2\rangle (\equiv |6, 2^*\rangle)$, we replaced $[R^{(t)}]$ in Eq.(D-2) by

$$\begin{bmatrix} 0 & 0 & 0 & 0 & 1 \\ 0 & 0 & 0 & 1 & 0 \\ 0 & 0 & 1 & 0 & 0 \\ 0 & 1 & 0 & 0 & 0 \\ 1 & 0 & 0 & 0 & 0 \end{bmatrix}.$$

However, in the convention of this paper, we take the basis functions for d-orbital as real functions, which means that $[R^{(t)}]$ must be identity. Accordingly, 5×5 matrices $[\vec{L}]$ in the spatial rotational operators should be taken as in eq.(21). As for the operators on the spin space, we take $\vec{S} = \frac{1}{2}\vec{\sigma}$.

$C(\vec{n}, \theta)^{-1}(i)$ in Eq.(D-3) represents the site which transports onto the site i when we apply the spatial rotation $C(\vec{n}, \theta)$. In contrast to the above operations, the spatial inversion I affects only on the site index i because the d -orbitals are always even under I ,

$$H_{(i,\mu,\alpha|j,\nu,\beta)} \rightarrow H_{(I(i),\mu,\alpha|I(j),\nu,\beta)}.$$

- 22) From the symmetry considerations, Dzyaloshinskii-Moriya (DM) interaction turns out to have no staggered components, while the uniform component of the DM vector is allowed to head for the z -direction. However, as far as canted AF spin con-

figurations are concerned, uniform components of DM vector do not matter.

- 23) Magnitudes of symmetric parts of anisotropic exchange interactions ΔJ are usually proportional to square of the spin-orbit coupling constant and thus very small.
- 24) Effects of depolarization (depolarizing) fields on the macroscopic electronic polarization (MEP) have been phenomenologically argued in the review article listed above.⁸
- 25) L.D.Landau, E.M.Lifshitz and L.P.Pitaevskii, *Electrodynamics of Continuous Media*, (Butterworth-Heinemann, 1985)
- 26) $\bar{J}_{\text{el}}(x)$ is defined by the time-dependent ground state wavefunction $|\Psi(t)\rangle$:

$$\bar{J}_{\text{el}}(x) \equiv \int_{-\infty}^0 dt \langle \Psi(t) | J_{\text{el}}(x) | \Psi(t) \rangle. \quad (\text{D}\cdot 4)$$

This ground state wave function $|\Psi(t)\rangle$ is now adiabatically evolved according to the time-dependent Hamiltonian given in eq.(A·2), where an infinitesimal perturbation $\delta\vec{\varphi}$ is introduced during the interval $t \in [-\infty, 0]$.

- 27) The inhomogeneity of the current distribution around sample boundaries, i.e. $x \pm \frac{L}{2}$, does not matter with our arguments, when L is taken to be sufficiently large.
- 28) In order to take into account the spatial variation of this depo-

larization field accurately, we need to solve the following self-consistent equation for $\bar{J}_{\text{el}}(x)$ instead of eq. (37):

$$\begin{aligned} \bar{J}_{\text{el}}(x) = & -\frac{i}{V} \sum_{m \neq 0} \left[\frac{\langle \Psi_0 | J_{\text{el}}(x) | \Psi_m \rangle \langle \Psi_0 | \delta H_{\text{M.F.}} | \Psi_m \rangle}{(E_m - E_0)^2} - \text{c.c.} \right] \\ & + \frac{ie}{\epsilon_0 V} \sum_{j=1}^N \sum_{m \neq 0} \left[\frac{\langle \Psi_0 | J_{\text{el}}(x) | \Psi_m \rangle \langle \Psi_0 | x_j | \Psi_m \rangle}{(E_m - E_0)^2} - \text{c.c.} \right] \bar{J}_{\text{el}}(x_j). \quad (\text{D}\cdot 5) \end{aligned}$$

Then, by integrating $\bar{J}_{\text{el}}(x)$ w.r.t. x , we obtain δP_{el} which is exact at the mean-field level.

- 29) Accurately speaking, rewriting the first term in the r.h.s. of eq.(33) into that of eq.(37) is allowed only in those situations where an electro-static field is absent *before* the perturbation $\delta\vec{\varphi}$ is introduced. Namely, eq. (37) and also (38) is valid only when experiments are performed in the following sequences: (i) Firstly, embed the system into some closed circuit (electric polarization in the system is short-circuited). (ii) Next, cut the electrodes (the system is now terminated without electrodes). (iii) Then, introduce an infinitesimal change of the spin ordering field $\delta\vec{\varphi}$ by applying magnetic fields.
- 30) T.Inui, Y.Tanabe, Y.Onodera, *Group Theory and Its Applications in Physics*, Solid State Sciences 78, chapter.13.